ICIC Express Letters
Part B: Applications
Volume **17**, Number **6**, June **2026**

pp. 623–630

NULL-NOISE SPECTRUM OF A 5G FUTURE DIGITAL TRANSMITTER SYSTEM

Dewiani Djamaluddin[1,*], Sirmayanti Sirmayanti[2] and Merna Baharuddin[1]

[1]Department of Electrical Engineering
Universitas Hasanuddin
Jl. Poros Malino Km. 6, Bontomarannu, Gowa, Sulawesi Selatan 92127, Indonesia
merna@unhas.ac.id
*Corresponding author: dewiani@unhas.ac.id

[2]Department of Electrical Engineering
The State Polytechnic of Ujung Pandang
Jalan Perintis Kemerdekaan Km. 10, Tamalanrea, Makassar 90245, Indonesia
sirmayanti.sirmayanti@poliupg.ac.id

Received October 2025; accepted December 2025

Abstract. *The urgent need to exploit additional usable spectrum in higher-frequency 5G bands, especially when these frequencies overlap with those used by 4G LTE, must be addressed to ensure efficient spectrum utilization. This paper proposes a distortion cancellation approach within the spectrum mask to optimize spectrum sharing while minimizing interference in 5G and beyond applications. The method employs a Sigma Delta ($\Sigma\Delta$) structure based on a radio frequency (RF) upconverter, designed to generate the desired signal with null-noise characteristics. The proposed architecture features a feedback filter unit using a Cartesian upconversion technique and incorporates a noise feedback loop that operates analogously to an analog-to-digital conversion (ADC) process. This loop iteratively adjusts until the quantized output matches the input signal, thereby achieving a null-noise state. Experimental results show that the spectrum of the OFDM signal achieves a 21 dB reduction down to the noise floor after the feedback filter's response, demonstrating both null-noise and symmetrical noise-shaping effects. Furthermore, a comparison between first-order (MOD1) and second-order (MOD2) $\Sigma\Delta$ modulators indicates that higher-order modulation and increased sampling rates can more effectively achieve null-noise at lower frequencies.*
Keywords: RF-spectrum, Cartesian-modulator, Null-noise, Noise-shaping, Sigma-Delta feedback

1. **Introduction.** Fifth-generation (5G) wireless technology, often described as Gigabit-per-second broadband communication, marks a major transition from 4G long term evolution (LTE) standards. According to the Federal Communications Commission (FCC), the 5G spectrum extends up to 100 GHz, with individual signal bandwidths exceeding 20 MHz [1-3]. However, despite this vast allocation, the rapid increase in capacity demand continues to challenge spectrum availability [4]. Service providers must utilize multiple frequency bands to support RF communication channels for both transmission and reception. As noted in [5], the 5G spectrum is divided into two main ranges: Range 1 (4.1-7.125 GHz), which serves conventional cellular traffic, and Range 2 (24.25-52.6 GHz), designated for high-data-rate, short-range applications. Consequently, optimizing the use of higher-frequency bands remains crucial to address ongoing spectrum scarcity.

In response to these challenges, current 4G spectrum implementations [6,7] are evolving toward integrated 4G-5G solutions. A study in [8] introduced a 60 GHz antenna-in-package (AIP) integrating full Tx-Rx functionality, providing high throughput and directivity but

DOI: 10.24507/icicelb.17.06.623

facing packaging constraints. To overcome such issues, a digital RF transmitter based on Sigma-Delta ($\Sigma\Delta$) modulation was proposed for 5G [9] to support low-latency IoT connectivity [10-13]. This digital signal processing (DSP)-based approach fosters green infrastructure and enhances reliability [14], flexibility [15], and linearity [16], as discussed in [13].

Building upon these advances, this study adopts the RF upconverter Cartesian structure described in [16,17] and the $\Sigma\Delta$ filter concept introduced in [9]. The proposed model employs polar-domain quantization to minimize spectral noise. Prior work in [18] proposed an iterative subtraction of quantization errors in the feedback loop until convergence, producing an error signal that separates signal and noise transfer functions (NTF) [19]. These principles collectively aim to improve spectral efficiency and enable robust 5G system design.

The present study specifically investigates noise-shaping behavior in the RF spectrum, focusing on achieving a null-noise condition. The Cartesian structure [16] demonstrates clear advantages over traditional bandpass and polar architectures, offering broader bandwidth [20] and reduced switching activity [21]. Nonetheless, even with baseband tuning methods designed to expand dynamic range, distortion issues persist in the RF spectrum [9,18]. Channel tuning with variable offsets can partially mitigate distortion, but a high noise floor remains when oversampling parameters are suboptimal [18].

To address these issues, this research extends previous work on $\Sigma\Delta$-based RF transmitter architectures [9,16-18], which have examined noise shaping, distortion suppression, and bandwidth expansion. However, earlier studies often treated these aspects separately, used oversampling methods that sustained high noise levels, and provided limited evaluation of feedback filters for null-noise generation. Moreover, the integration of these techniques within a Cartesian upconverter framework – particularly in comparing modulator orders has not been extensively explored. This study closes these gaps by implementing and analyzing a feedback filter unit within the Cartesian structure and comparing 1st- and 2nd-order $\Sigma\Delta$ modulators (MOD1 and MOD2). The goal is to demonstrate simultaneous null-noise generation and symmetrical noise shaping for efficient 5G spectrum sharing. The novelty lies in the iterative feedback loop, analogous to ADC operation, which converges the quantized output toward the input signal, achieving effective noise suppression and distortion control across both MOD1 and MOD2 configurations.

This paper is structured as follows. Section 1 introduces the digital RF transmitter architecture based on Sigma-Delta ($\Sigma\Delta$) modulation and its effectiveness in achieving noise shaping and distortion reduction. Section 2 outlines the problem statement, theoretical background, and proposed methodology. Section 3 details the experimental setup and presents the main results with analysis, while Section 4 discusses the findings and their implications for future 5G spectrum design.

2. **Problem Statement and Preliminaries.** This research employed MATLAB-based simulations for signal generation and modulator modeling, allowing flexible parameter testing. The orthogonal frequency division multiplexing (OFDM) modeling stage generated waveform inputs for the Cartesian $\Sigma\Delta$ structure, with a carrier frequency (f_c) of 2300 MHz aligned with 5G bands [22] and a corresponding sampling frequency (f_s). The in-phase and quadrature (I/Q) outputs from the OFDM stage were processed through a DSP module containing a $\Sigma\Delta$ low-pass filter (LPF) [14], quantizer, and pulse modulation stage to produce the final RF waveform, as illustrated in Figure 1.

The $\Sigma\Delta$-LPFs function to suppress noise floors and achieve effective noise shaping. Operating as digital modulators, $\Sigma\Delta$-LPFs replace analog components, eliminating hardware-related challenges [9]. Analog circuits such as local oscillator (LO) leakage, power amplifier

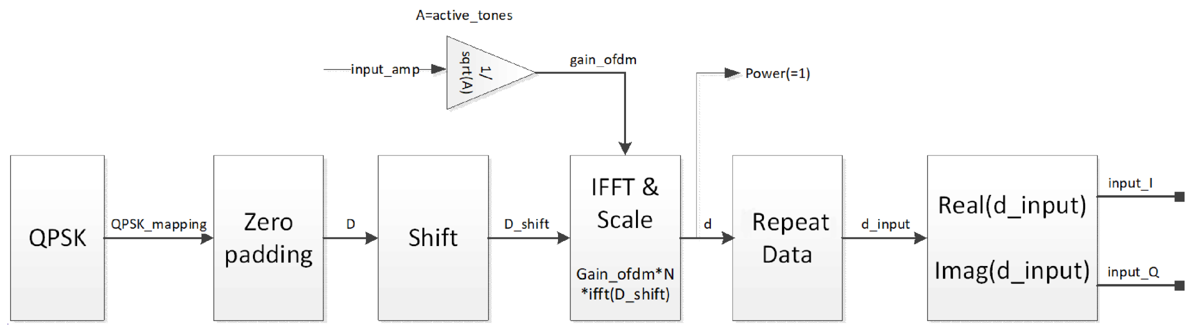

FIGURE 1. OFDM modelling with DSP module I/Q

(PA) nonlinearities, and I/Q imbalance are prone to distortion [23]. In this context, ΣΔ-LPFs mitigate such issues and address bandwidth limitations from PA nonlinearities in the transmitter (Tx) path [24], thus improving signal integrity and transmission efficiency.

Input I/Q signals from the DSP module pass through ΣΔ filters where ΣΔ-LPF blocks and feedback filters remain in Cartesian format, while subsequent RF stages operate in the polar domain [9]. Continuous subtraction of quantization errors enhances fidelity, with ΣΔ-LPFs supporting oversampling and noise shaping. This configuration ensures high linearity and wideband performance for 5G signal generation.

A study using a single undersampling ADC [25] reported lower normalized mean square error (MSE) when paired with digital predistortion. Similarly, common-mode feedback units in single-ended or differential converters enable low-power operation and efficiency [26]. These findings highlight that ΣΔ-based converters effectively balance digital correction and power optimization.

The Cartesian ΣΔ modulator redistributes quantization noise across the spectrum, minimizing it near the target band [27]. Unlike polar ΣΔ modulators [28], which increase noise through amplitude-phase separation, the Cartesian approach doubles I/Q bandwidth via oversampling [29], thus reducing quantization noise [19] and enhancing spectral efficiency, crucial for 5G waveform fidelity.

A first-order ΣΔ modulator (MOD1), functioning as a ΣΔ-LPF, is modeled in the z-domain, with the quantizer (Q) integrated within the feedback loop to minimize noise and improve signal quality. Based on MOD1, higher-order ΣΔ modulators enhance noise shaping and design stability, especially when using a single quantizer to avoid overload. Cascaded ΣΔ-LPFs further suppress quantization noise, making them suitable for low-frequency digital to analog converter (DAC) applications.

The second-order MOD2 structure, formed by cascading two MOD1 stages, improves linearity, especially with a two-level DAC [30], while enabling adjustable oversampling ratios and higher modulator orders. An infinite impulse response (IIR) feedback loop increases dynamic range and improves linearity through magnitude attenuation. Prior studies [31-34] confirm that DAC-based ΣΔ structures provide effective noise shaping, better bit error rate (BER) tolerance, and minimal error vector magnitude (EVM) degradation, validating the proposed digital transmitter design for 5G systems.

3. **Main Results.** The ΣΔ LPFs are commonly analyzed within a linear model for mathematical evaluations [9,27]. In this framework, the $H(z)$ function represents the filter (integrator) in the z-domain, with a transfer function of z^{-1}. The system controls (i) noise shaping $E(z)$ through the NTF, and (ii) signal filtering via the signal transfer function (STF) from the module 1/Q input. When the direct current (DC) gain in the integrator approaches infinity, white noise at DC emerges. Higher-order digital filters $H(z)$ contribute more effectively to noise shaping within the circuit. Referring to the modeling results for MOD1 presented in Figure 2, the feedback filter spectrum shows two

phenomena: null-noise and noise shaping. The OFDM band of interest is visible at the carrier frequency (f_c) on the spectrum, with a 21 dB reduction in the noise floor following the feedback filter response. Null-noise occurs when the band sits at the lowest point in the spectrum. Additionally, the spectrum demonstrates more symmetric noise shaping and a stronger null-noise effect around the targeted frequency band.

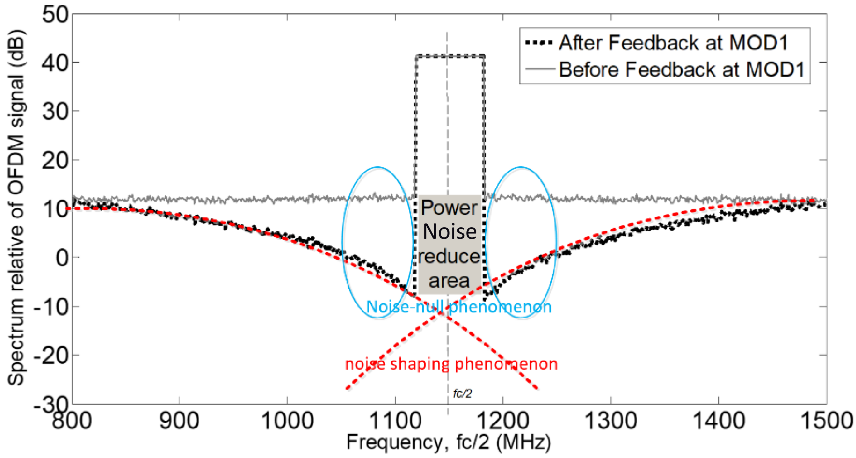

FIGURE 2. Feedback filter responds to MOD1

Figure 3 plots the noise shaping performance between MOD1 and MOD2 corresponding to an oversampling ratio (OSR = 16). The noise shaping of MOD1 is higher than MOD2 in the spectrum mask (near DC), however, the quantization noise power spectrum density (PSD) of MOD1 is much lower and performs the derivative deeper about 8 dB better to MOD2.

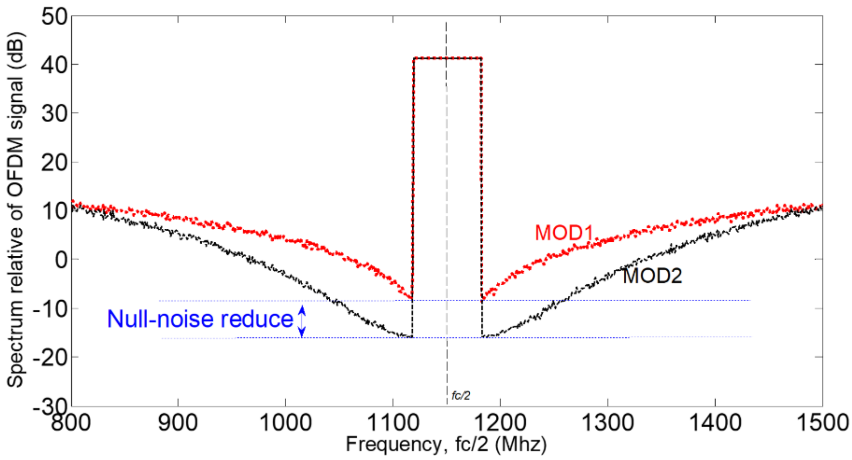

FIGURE 3. Noise shaping between MOD1 and MOD2

Assume $f \ll 1$ (let us set $f = 0$), so $|NTF_{MOD1}|^2 = |NTF_{MOD2}|^4 \approx 0$ is for normalized frequencies. This will indicate that $\Sigma\Delta$ LPF characteristic has effectiveness at the lower frequency area, in which the action of quantization noise can be shifted or removed from the targeted signal as consequence of the noise shaping filter operation.

A study in [19] identifies two key approaches for ensuring the stability of digital filter designs: (i) placing zeros to achieve null-noise and (ii) placing poles to facilitate noise shaping, thereby minimizing potential noise enhancement while maintaining stability. This is quantified by the modified Lee criterion, which ensures that the maximum magnitude of the frequency response $\mathbf{max}_\omega \left| H\left(e^{j\omega}\right) \right| < 1.5$ for stability and filtering considerations.

In this context, the placement of poles and zeros in the NTF governs the effectiveness of noise shaping. Consequently, the relationship between the STF, NTF, and the overall transfer function $H(z)$ is given by $STF(z) = 1 - NTF(z)$.

Figure 4 illustrates the NTF and STF characteristics for both MOD1 and MOD2, showing their effects on the spectrum. Theoretically, the NTF of MOD2 exhibits lower noise levels compared to MOD1, and both STFs remain stable for DC signals. When this approach is implemented within the Cartesian structure, the feedback filter continuously loops the sampled bit-input signal, ensuring that the resulting quantized signal matches the input. By increasing the OSR and applying second-order (MOD2) $\Sigma\Delta$ filters, it is possible to achieve a better null-noise effect in the spectrum. In most RF upconverter applications, the MOD2 structure is typically preferred due to its superior noise shaping performance.

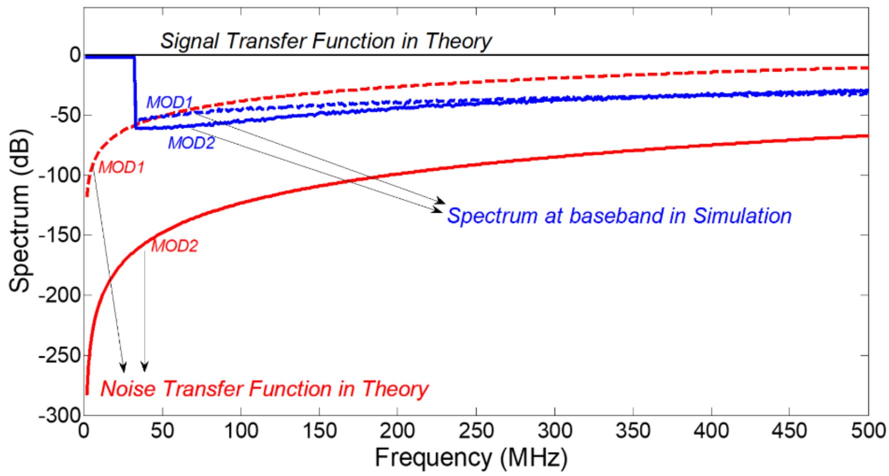

Figure 4. NTF and STF MOD1 and MOD2 effects in the spectrum

The level amplitude size (N_A) is calculated by OSR, so that given

$$N_A = \frac{OSR}{4} + 1 \tag{1}$$

where OSR is the number of phases N_P, or can be written by

$$N_P = OSR \tag{2}$$

The level amplitude size of N_A describes the total number of quantization points; therefore,

$$N_A = OSR\left(\left(\frac{OSR}{4}\right) + 1\right) \tag{3}$$

The quantized phase, $\hat{v}_\theta$, is given by

$$\hat{v}_\theta = (\tau_p + 0.5)\frac{2\pi}{N_P} \tag{4}$$

where the position of the pulse (τ_p) represents the time delay, and this indicates the pulse position modulation (PPM) delay in the clock period. τ_p values 0 to $(N_P - 1)$.

Furthermore, the fundamental amplitude of the pulse wave can be defined

$$\hat{v}_r(\delta) = 2[|U_{n=1}(\delta, \tau_p, OSR)|] \tag{5}$$

where $n = 1$ indicates the first frequency bin from a discrete Fourier transform (DFT), and δ is the pulse-wave width corresponding to the clock cycles.

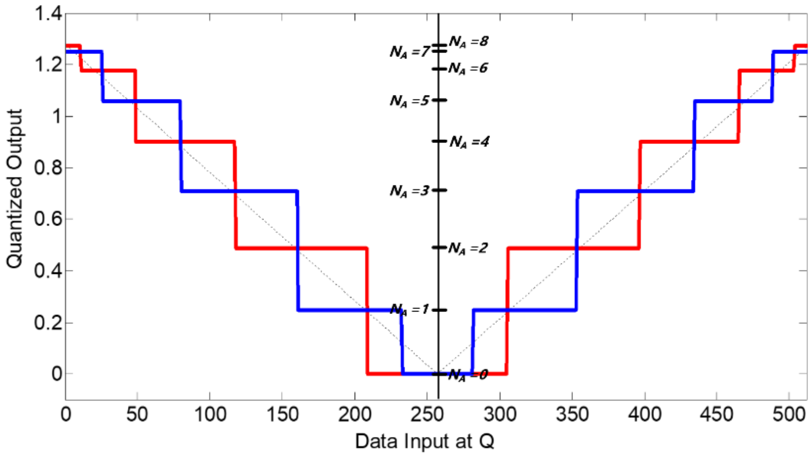

FIGURE 5. A stepped triangle wave for quantization levels of the quantized amplitude ($\hat{v}_r$) vs input amplitude (v_r)

In Figure 5, a mathematical analysis approach is employed that considers the partition between odd and even pulse widths. This means that every two sample increments (whether odd or even) serve to separate the amplitude response from the phase response. Each pulse width step size is designed to maintain symmetry around a central reference point. Subsequently, the initial three-level waveform spectral components of the I/Q signals for each amplitude increment are calculated, converting to the values 1, 0, and −1.

4. **Conclusions.** In conclusion, the OSR strongly affects quantization levels and RF output power. The proposed DSP-based RF upconverter efficiently manages sampling rates, where higher rates expand the NTF bandwidth and enable null-noise targeting. The Cartesian feedback loop accelerates quantization, minimizing small errors. These noise-shaping effects effectively mitigate interference in frequency sharing. However, offsetting methods may introduce distortion. Adjusting clock frequency to isolate desired bands can help, though it increases filter design and PA complexity, indicating the need for further optimization in future studies.

Acknowledgment. The authors gratefully acknowledge the 5G Research Group of Hasanuddin University for funding support through the PDUH scheme and the CATTAR Research Group of the State Polytechnic of Ujung Pandang for their valuable collaboration.

REFERENCES

[1] A. N. Uwaechia and N. M. Mahyuddin, A comprehensive survey on millimeter wave communications for fifth-generation wireless networks: Feasibility and challenges, *IEEE Access*, vol.8, pp.62367-62414, 2020.

[2] J. Zhang, P. Tang, L. Tian, Z. Hu, T. Wang and H. Wang, 6-100 GHz research progress and challenges from a channel perspective for fifth generation (5G) and future wireless communication, *Science China Information Sciences*, vol.60, no.8, 2017.

[3] Federal Communications Commission, *Spectrum Frontiers Report and Order and Further Notice of Proposed Rulemaking: FCC16-89*, https://docs.fcc.gov/public/attachments/FCC-16-89A1.pdf, 2016.

[4] F. Hu et al., Full spectrum sharing in cognitive radio networks toward 5G: A survey, *IEEE Access*, vol.6, pp.15754-15776, 2018.

[5] R. Dilli, Analysis of 5G wireless systems in FR1 and FR2 frequency bands, *The 2nd International Conference on Innovative Mechanisms for Industry Applications, ICIMIA 2020 – Conference Proceedings*, pp.767-772, 2020.

[6] L. Wan et al., 4G/5G spectrum sharing: Efficient 5G deployment to serve enhanced mobile broadband and Internet of Things applications, *IEEE Vehicular Technology Magazine*, vol.13, no.4, pp.28-39, 2018.

[7] W. A. Hassan, H. S. Jo, S. Ikki and M. Nekovee, Spectrum-sharing method for co-existence between 5G OFDM-based system and fixed service, *IEEE Access*, vol.7, pp.77460-77475, 2019.

[8] Z. Fang et al., Integrated wideband chip-scale RF transceivers for radar sensing and UWB communications: A survey, *IEEE Circuits and Systems Magazine*, vol.22, no.1, pp.40-76, 2022.

[9] A. Spelman, *System Modeling for 5G Integrated Digital Transmitters*, https://aaltodoc.aalto.fi/server/api/core/bitstreams/8cb5cfd6-9e57-457c-b576-f22f7d007bea/content, 2021.

[10] B. S. Awoyemi, A. S. Alfa and B. T. Maharaj, Resource optimisation in 5G and Internet-of-Things networking, *Wireless Personal Communications*, vol.111, pp.2671-2702, 2020.

[11] M. U. Hadi, A. Basit and K. Khurshid, MIMO enabled multiband 5G NR fiberwireless using Sigma Delta over fibertechnology, *IEEE 2021 International Bhurban Conference on Applied Sciences and Technologies (IBCAST)*, pp.1007-1010, 2021.

[12] D. Klonidis et al., Int5Gent: An integrated end-to-end system platform for verticals and data plane solutions beyond 5G, *IEEE 2021 Joint European Conference on Networks and Communications & 6G Summit (EuCNC/6G Summit)*, pp.604-609, 2021.

[13] A. Jerng and C. G. Sodini, A wideband $\Delta\Sigma$ digital-RF modulator for high data rate transmitters, *IEEE Journal of Solid-State Circuits*, vol.42, no.8, pp.1710-1722, 2007.

[14] S. Sirmayanti and M. Faulkner, $\Sigma\Delta$ modulator for digital wireless architecture: A review, *IEEE Makassar International Conference on Electrical Engineering and Informatics (MICEEI)*, pp.83-87, 2014.

[15] M. Helaoui, S. Hatami, R. Negra and F. M. Ghannouchi, A novel architecture of Delta-Sigma modulator enabling all-digital multiband multistandard RF transmitters design, *IEEE Transactions on Circuits and Systems II: Express Briefs*, vol.55, no.11, pp.1129-1133, 2008.

[16] V. Bassoo and M. Faulkner, Sigma-Delta digital drive signals for switch-mode power amplifiers, *Journal of Electronics Letters*, vol.44, pp.1299-1300, 2009.

[17] H. Ruotsalainen, H. Arthaber and G. Magerl, A new quadrature PWM modulator with tunable center frequency for digital RF transmitters, *IEEE Transactions on Circuits and Systems II: Express Briefs*, vol.59, pp.756-760, 2012.

[18] S. Sirmayanti and M. Faulkner, Tuning baseband on Cartesian Delta-Sigma up-conversion, *IET e-Letters Journal*, vol.50, no.8, pp.635-637, 2014.

[19] R. Schreier, G. C. Temes and J. Wiley, *Understanding Delta-Sigma Data Converters*, IEEE Press, Piscataway, NJ, 2005.

[20] H. Sjöland, C. Bryant, V. Bassoo and M. Faulkner, Switched-mode transmitter architectures, in *Analog Circuit Design*, A. Roermund, H. Casier and M. Steyaert (eds.), Dordrecht, Springer, 2010.

[21] M. Nielsen and T. Larsen, A transmitter architecture based on Delta-Sigma modulation and switch-mode power amplification, *IEEE Transactions on Circuits and Systems II: Express Briefs*, vol.54, pp.735-739, 2007.

[22] A. Wulandari, M. Hasan, A. Hikmaturokhman, Ashamdono, L. Damayanti and Damelia, 5G stand alone inter-band carrier aggregation planning in Kelapa Gading Jakarta Utara, *Proc. of IEEE 2nd International Conference on ICT for Rural Development, IC-ICTRuDev*, pp.1-6, 2021.

[23] Y. Yao, Y. Jin, M. Li, Z. Dai and S. He, An accurate three-input nonlinear model for joint compensation of frequency-dependent I/Q imbalance and power amplifier distortion, *IEEE Access*, vol.7, pp.140651-140664, 2019.

[24] B. Kang, Y. Fan and Y. Gao, Wideband photonic image-reject RF receiver based on phase modulation and I/Q balanced detection, *IEEE International Topical Meeting on Microwave Photonics (MWP)*, pp.1-4, 2019.

[25] M. Almoneer, P. Mitran and S. Boumaiza, I/Q imbalance compensation in wideband millimeter-wave transmitters using a single undersampling ADC, *IEEE Transactions on Circuits and Systems I: Regular Papers*, vol.67, no.8, pp.2730-2738, 2020.

[26] T. He et al., Noise filtering and linearization of single-ended sampled-data circuits, *IEEE Transactions on Circuits and Systems I: Regular Papers*, vol.66, no.4, pp.1331-1341, 2019.

[27] N. E. Majd and A. Aeenmehr, Efficiency improvement of Delta Sigma modulator-based transmitter using complex Delta Sigma modulator and noise reduction loop, *Journal of Circuits, Systems and Computers*, vol.29, no.16, 2050267, 2020.

[28] V. Bassoo, A. Mustafa and M. Faulkner, Distortion arising from polar to PWM/PPM conversion in an all digital upconverter for switching RF power amplifier, *IEEE MTT-S International Microwave Symposium Digest*, pp.1533-1536, 2009.

[29] F. T. Gebreyohannes et al., All-digital transmitter architecture based on two-path parallel 1-bit high pass filtering DACs, *IEEE Transactions on Circuits and Systems I: Regular Papers*, vol.65, no.11, pp.3956-3969, 2018.

[30] B. P. Brandt, D. E. Tvingard and B. A. Wooley, Second-order Sigma-Delta modulation for digital-audio signal acquisition, *IEEE Journal of Solid-State Circuits*, vol.26, no.4, pp.618-627, 1991.

[31] J. H. Park et al., A VCO-based 2nd order 2-Σ modulator for small-size high energy-efficient current sensing front-end, *IEEE Solid-State Circuits Letters*, vol.6, pp.92-96, 2023.

[32] M. Shao, W. K. Ma and L. Swindlehurst, Multiuser massive MIMO downlink precoding using second-order spatial Sigma-Delta modulation, *IEEE International Conference on Acoustics, Speech and Signal Processing (ICASSP)*, pp.8966-8970, 2020.

[33] J. Wang et al., Digital mobile fronthaul based on Delta-Sigma modulation for 32 LTE carrier aggregation and FBMC signals, *Journal of Optical Communications and Networking*, vol.9, no.2, pp.A233-A244, 2017.

[34] J. Wang, Z. Jia, L. A. Campos and C. Knittle, Delta-Sigma digitization and optical coherent transmission of DOCSIS 3.1 signals in hybrid fiber coax networks, *Fiber Optics – From Fundamentals to Industrial Applications*, IntechOpen, 2019.